Adaptive accurate tracking control of HFVs in the presence of dead-zone and hysteresis input nonlinearities

Dong, Zehong; LI, Yinghui; LV, Maolong; Zuo, Renwei

DOI
10.1016/j.cja.2020.10.028

Publication date
2021

Document Version
Final published version

Published in
Chinese Journal of Aeronautics

Chinese Journal of Aeronautics, (2021), **34**(5): 642–651

Chinese Society of Aeronautics and Astronautics
& Beihang University

Chinese Journal of Aeronautics

cja@buaa.edu.cn
www.sciencedirect.com

Adaptive accurate tracking control of HFVs in the presence of dead-zone and hysteresis input nonlinearities

Zehong DONG [a,b], **Yinghui LI** [b,*], **Maolong LV** [a,c], **Renwei ZUO** [a,b]

[a] *Graduate College, Air Force Engineering University, Xi'an 710100, China*
[b] *Aeronautics Engineering College, Air Force Engineering University, Xi'an 710038, China*
[c] *Delft Center for Systems and Control, Delft University of Technology, Mekelweg 2, Delft 2628 CD, The Netherlands*

Received 11 June 2020; revised 20 August 2020; accepted 19 October 2020
Available online 12 January 2021

KEYWORDS

Accurate tracking control;
Back-stepping control;
Dead-Zone and hysteresis;
Hypersonic flight vehicles;
Non-affine model

Abstract A novel accurate tracking controller is developed for the longitudinal dynamics of Hypersonic Flight Vehicles (HFVs) in the presence of large model uncertainties, external disturbances and actuator nonlinearities. Distinct from the state-of-the-art, besides being continuity, no restrictive conditions have been imposed on the HFVs dynamics. The system uncertainties are skillfully handled by being seen as bounded "disturbance terms". In addition, by means of back-stepping adaptive technique, the accurate tracking (i.e. tracking errors converge to zero as time approaches infinity) rather than bounded tracking (i.e. tracking errors converge to residual sets) has been achieved. What's more, the accurate tracking problems for HFVs subject to actuator dead-zone and hysteresis are discussed, respectively. Then, all signals of closed-loop system are verified to be Semi-Global Uniformly Ultimate Boundness (SGUUB). Finally, the efficacy and superiority of the developed control strategy are confirmed by simulation results.

* Corresponding author.
E-mail address: liyinghui66@163.com (Y. LI).
Peer review under responsibility of Editorial Committee of CJA.

Production and hosting by Elsevier

https://doi.org/10.1016/j.cja.2020.10.028
1000-9361 © 2021 Chinese Society of Aeronautics and Astronautics. Production and hosting by Elsevier Ltd.

V	Velocity	h	Altitude
θ	Pitch angle	γ	Flight path angle
α	Angle of attack	Q	Pitch rate
T	Thrust	D	Drag
L	Lift	M	Pitching moment
I_{yy}	Moment of inertia	m	Vehicle mass
Φ	Fuel equivalence ratio	δ_e	Elevator angular deflection
N_i	$i$thgeneralized force	η_i	ith generalized flexible coordinate
$\tilde{\psi}_i$	Constrained beam coupling constant for η_i	ζ_i	Damping ratio for flexible mode η_i
ω_i	Natural frequency for flexible mode η_i	$N_i^{\alpha^j}$	jth order contribution of α to N_i
N_i^0	Constant term in N_i	$N_2^{\delta_e}$	Contribution of δ_e to N_2
$C_D^{\alpha^i}$	ith order coefficient of α in D	$C_D^{\delta_e^i}$	ith order coefficient of δ_e in D
C_D^0	Constant term in D	$C_L^{\alpha^i}$	ith order coefficient of α in L
$C_L^{\delta_e}$	Coefficient of δ_e in L	C_L^0	Constant term in L
$C_{M,\alpha}^{\alpha^i}$	ith order coefficient of α in M	$C_{M,\alpha}^0$	Constant term in M
c_e	Coefficient of δ_e in M	$\beta_i(h,\bar{q})$	ith thrust fit parameter
z_T	Thrust moment arm	h_0	Nominal altitude for air density approximation
$\bar{c}$	Mean aerodynamic chord	$\bar{q}$	Dynamic pressure
$\bar{\rho}$	Air density	$\bar{\rho}_0$	Air density at the altitude h_0
$1/h_s$	Air density decay rate	S	Reference area

1. Introduction

Hypersonic Flight Vehicles (HFVs) have attracted more and more attention recently on account of the high speed and high cost performance, processing great military and civilian values. In recent years, tremendous efforts including model investigation and controller design in Refs.[1–15] have been made. It is worth noting that there exist strong uncertainties in HFVs dynamics due to the strong dynamics coupling, fast time-varying flight environment and unknown actuator nonlinearities.[5,10] In addition, the integration of the propulsion system and the body enhances the dynamics coupling characteristics and nonlinearities, making the controller design for HFVs more complicated.[13]

In order to deal with the large system uncertainties in HFVs dynamics, numerous control methodologies have been proposed, including robust control,[5,6] sliding mode control,[8–10] intelligent control,[11,12] prescribed performance control,[13–15] etc. These literatures have made great contributions to HFVs research. From a practical perspective, a key issue that may be often encountered is that the control inputs cannot be implemented accurately because of actuator input nonlinearity.[16] However, the aforementioned works did not take into full consideration the actuator input nonlinearities such as dead-zone and backlash due to the existence of hydraulic actuator and hinge. In practice, the existence of actuator nonlinearity not only degrades the control accuracy and the flight performance, but even causes system instability in severe case.[17] With the development of HFVs control technique, the issues of actuator input nonlinearity are getting more and more attention in controller design. To list a few, an adaptive fault-tolerant control strategy is addressed to deal with the issue of input saturation and actuator fault in Ref.[18] Nevertheless, the dead-zone and hysteresis nonlinearities are not addressed therein. In Ref.[19] a neuro-adaptive approach is presented to cope with the problem of unknown actuator dead-zone for switched stochastic nonlinear systems, where the uncertainties of system are estimated by radial basis function neural networks (RBFNNs). An observer-based adaptive controller is address to eliminate the unfavorable effect caused by actuator dead-zone and hysteresis in Ref.[20] where the unknown dynamics are approximated via fuzzy logic systems.[21] In Ref.[22] RBFNNs are introduced to estimate the dynamic uncertainties caused by the input constraints and external disturbances. What's more, an improved performance function is proposed so as to guarantee some predefined transient and steady state attributes in the presence of dead-zone in Ref.[23]

Unfortunately, to our best knowledge, the above-mentioned literatures are merely able to achieve bounded tracking, i.e., tracking errors converge to a residual set whose size relies on some unknown design parameters. In other words, accurate tracking control for HFVs has not been investigated in state-of-the-art. Noting that accurate tracking for HFVs is of paramount importance in practice, such as large maneuver flight,[24] precision strike,[25] and so on. More recently, some accurate tracking control methodologies are proposed for nonlinear systems.[26–28] In Ref.[26] a novel adaptive filter for the nonlinear hysteretic system is addressed to implement the accurate tracking for reference trajectory. Furthermore, Ref.[27] exploits an adaptive asymptotic control scheme for pure-feedback system, in which the form of model is transformed from non-affine to affine by defining a novel function. Nevertheless, owing to the existence of unmodeled dynamics, fast time-varying flight environment and external disturbances of HFVs, these accurate tracking control methods cannot be applied directly to the HFVs, especially when the unknown dead-zone and hysteresis nonlinearities appear.[16,23] Therefore,

how to design an accurate tracking controller for HFVs in the presence of dead-zone and hysteresis nonlinearities needs to be clearly exploited.

In recent years, Back-Stepping Control (BSC), which is perceived as a direct effective mean to design the controllers for nonlinear systems,[29–31] is generally applied for implementing tracking control for HFVs.[32] Motivated by above observations, this work develops a back-stepping adaptive accurate tracking control for HFVs in spite of actuator dead-zone and hysteresis nonlinearities. The main contributions of this article are as follows:

(1) To the best of authors' knowledge, this might be a pioneering work achieving accurate tracking for HFVs subject to uncertain dead-zone and hysteresis nonlinearities. Compared with most of available researches on HFVs in Refs.[6,7] and Refs.[13–17] the velocity and altitude tracking errors can accurately converge to zero rather than a residual set.
(2) In contrast to the conventional adaptive neural control in Refs.[7,13,33] the neural networks are removed and only one parameter needs to be updated in each control law. Thus, the proposed method is simpler and can reduce the computational burden in theory.
(3) In comparison with Ref.[23] and Refs.[34,35], a novel zero-errors tracking control scheme for HFVs is further presented against the system uncertainties caused by actuator nonlinearity and external disturbance, where the system uncertainties are skillfully disposed by being regarded as bounded "disturbance terms".

The remainder of this paper is organized as follows. In Section 2, model description and preliminaries are provided. Then, the controller design process is given in Section 3 and the close-loop stability is analyzed in Section 4. In Section 5, simulation results are presented to prove the effectiveness of the proposed scheme and the conclusions are included in Section 6.

2. Model description and preliminaries

2.1. Longitudinal dynamics of HFVs

The longitudinal dynamic model of HFVs is considered as[36]

$$\begin{cases} \dot{V} = \frac{T\cos(\theta-\gamma)-D}{m} - g\sin\gamma \\ \dot{h} = V\sin\gamma \\ \dot{\gamma} = \frac{T\sin(\theta-\gamma)+L}{mV} - \frac{g\cos\gamma}{V} \\ \dot{\theta} = Q \\ \dot{Q} = \frac{M+\tilde{\psi}_1\ddot{\eta}_1+\tilde{\psi}_2\ddot{\eta}_2}{I_{yy}} \\ k_1\ddot{\eta}_1 = -2\zeta_1\omega_1\dot{\eta}_1 - \omega_1^2\eta_1 + N_1 - \frac{\tilde{\psi}_1 M}{I_{yy}} - \frac{\tilde{\psi}_1\tilde{\psi}_2\ddot{\eta}_2}{I_{yy}} \\ k_2\ddot{\eta}_2 = -2\zeta_2\omega_2\dot{\eta}_2 - \omega_2^2\eta_2 + N_2 - \frac{\tilde{\psi}_2 M}{I_{yy}} - \frac{\tilde{\psi}_2\tilde{\psi}_1\ddot{\eta}_1}{I_{yy}} \end{cases} \tag{1}$$

where T, D, L, M, N_1 and N_2 can be formulated as

$$\begin{cases} T \approx \beta_1(h,\bar{q})\delta_\Phi\alpha^3 + \beta_2(h,\bar{q})\alpha^3 + \beta_3(h,\bar{q})\delta_\Phi\alpha^2 \\ \quad +\beta_4(h,\bar{q})\alpha^2 + \beta_5(h,\bar{q})\delta_\Phi\alpha + \beta_6(h,\bar{q})\alpha \\ \quad +\beta_7(h,\bar{q})\delta_\Phi + \beta_8(h,\bar{q}) \\ D \approx \bar{q}SC_D^{\alpha^2}\alpha^2 + \bar{q}SC_D^{\alpha}\alpha + \bar{q}SC_D^{\delta_e^2}\delta_e^2 + \bar{q}SC_D^{\delta_e}\delta_e + \bar{q}SC_D^0 \\ M \approx z_T T + \bar{q}S\bar{c}C_{M,\alpha}^{\alpha^2}\alpha^2 + \bar{q}S\bar{c}C_{M,\alpha}^{\alpha}\alpha + \bar{q}S\bar{c}C_{M,\alpha}^0 + \bar{q}S\bar{c}c_e\delta_e \\ L \approx \bar{q}SC_L^{\alpha}\alpha + \bar{q}SC_L^{\delta_e}\delta_e + \bar{q}SC_L^0 \\ N_1 = N_1^{\alpha^2}\alpha^2 + N_1^{\alpha}\alpha + N_1^0 \\ N_2 = N_2^{\alpha^2}\alpha^2 + N_2^{\alpha}\alpha + N_2^{\delta_e}\delta_e + N_2^0 \\ \bar{q} = \frac{\bar{\rho}V^2}{2}, \qquad \bar{\rho} = \bar{\rho}_0\exp\left(\frac{h_0-h}{h_s}\right) \end{cases} \tag{2}$$

where the more detailed definitions can be consulted in Refs.[36,37]

2.2. Actuator nonlinearities

During the flight, the actuators of HFVs may present uncertain nonlinearities, which significantly increase the difficulty of controller design and threaten the flight safety. The actuator model is considered as $\vartheta = \upsilon(u)$ where u and ϑ denotes the input and output of actuator, respectively, $\upsilon(\cdot)$ is an unknown nonlinear function. In this work, two negative characteristics of actuator, dead-zone and hysteresis, are taken into accountant.

The dead-zone model is described as follow[38]

$$\upsilon(u) = \begin{cases} k_r(u-u_a), & u > u_a \\ 0, & u_b \leqslant u \leqslant u_a \\ k_l(u-u_b), & u < u_b \end{cases} \tag{3}$$

where u_a and u_b denote breakpoints of the dead-zone model, k_l and k_r represent left and right slope of dead-zone nonlinearity. The hysteresis characteristic is described by the Bouc-Wen model as[26]

$$\begin{cases} \upsilon(u) = abu + (1-a)b\ell \\ \dot{\ell} = \dot{u} - c|\dot{u}|\,|\ell|^{n-1} - \omega\dot{u}\,|\ell|^n \end{cases} \tag{4}$$

where c and ω are constants depicting the shape and amplitude of the hysteresis and the readers can refer to Ref.[26] for more details. The curves of the Eqs. (3) and (4) are depicted in Fig. 1, where the parameters are set as $k_r = k_l = 10/9$, $u_a = 0.1$, $u_b = -0.1$, $a = 1/3$, $b = 3$, $c = 1$, $\omega = 0.5$, $\ell(0) = 0$, $u(t) = 4\sin(2t)$.

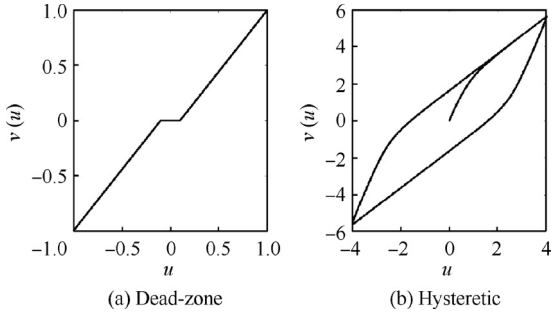

Fig 1 Dead-zone and hysteresis characteristics.

Remark 1. *In fact, it is worth noting that actuator nonlinearities as dead zone and hysteresis exist in a wide range of HFVs due to the electronic circuits, hydraulic servo values and mechanical connections.*[23] *To make matters worse, the dead zone and hysteresis nonlinearities may induce deterioration of the system performance even lead to instability of the closed-loop system.*[39] *Thus, it is extremely meaningful to exploit the control for HFVs in the case of dead zone and hysteresis nonlinearities.*

2.3. Model transformation and decomposition

It can be seen from Eqs. (1) and (2) that V is mainly related to Φ and h is mainly governed by δ_e, respectively.[13] Thus, in order to simplify the controller design, the HFVs dynamics are decomposed into velocity subsystem and altitude subsystem in this work. Inspired by Refs.[13,40] the velocity subsystem is considered as

$$\dot{V} = f_V + g_V \upsilon(\Phi) + d_V \tag{5}$$

where $f_V = \left(\overline{q}SC_D^{\alpha^2}\alpha^2 + \overline{q}SC_D^0\right)/m + \cos\alpha[\beta_2(h,\overline{q})\alpha^3 + \beta_4(h,\overline{q})\alpha^2 + \beta_6(h,\overline{q})\alpha + \beta_8(h,\overline{q})]/m - g\sin\gamma, g_V = \cos\alpha[\beta_7(h,\overline{q}) + \beta_3(h,\overline{q})\alpha^2 + \beta_1(h,\overline{q})\alpha^3]/m$. The functions f_V and g_V are considered to be uncertain.[6] $\upsilon(\Phi)$ represents the uncertain nonlinear of Φ; d_V is the lumped perturbation on velocity resulting from aerodynamic coefficients uncertainties and external disturbances.

Remark 2. *During the flight, the aerodynamic parameters will change with the variation of flight environment, the functions f_V and g_V are affected by the aerodynamic parameters. Indeed, an exact model for HFVs is difficult to be obtained since the complex flight environment of HFVs is hard to be reproduced in a wind tunnel.*[6] *In order to increase the robustness of system, we regard f_V and g_V as unknown functions.*

On account of the fact that γ is fairly small during cruise phase, so the approximations $\sin\gamma \approx \gamma$ and $\cos\gamma \approx 1$ stand,[41] then the velocity subsystem can be formulated as

$$\begin{cases} \dot{h} = V\gamma + d_h \\ \dot{\gamma} = f_\gamma + g_\gamma\theta + d_\gamma \\ \dot{\theta} = Q \\ \dot{Q} = f_Q + g_Q\upsilon(\delta_e) + d_Q \end{cases} \tag{6}$$

where

$$f_\gamma = \frac{\overline{q}S\left(C_L^0 - C_L^\alpha\gamma\right) + T\sin\alpha}{mV} - \frac{g}{V},\quad g_\gamma = \frac{\overline{q}SC_L^\alpha}{mV},$$

$$f_Q = z_T T + \frac{\overline{q}S\overline{c}C_{M,\alpha}(\alpha)}{I_{yy}},\quad g_Q = \frac{\overline{q}S\overline{c}c_e}{I_{yy}}.$$

Similarly to velocity subsystem, the functions f_γ, g_γ, f_Q and g_Q are unknown and $\upsilon(\delta_e)$ represents the uncertain nonlinearity of δ_e. d_h, d_γ, d_θ and d_Q are the lumped perturbations on altitude, flight path angle and pitch rate resulting from aerodynamic coefficients uncertainties and external disturbances, respectively.

Assumption 1. [37] *The sign of g_* is assumed to be known. Further, there exist positive functions $f_{*\mathrm{M}}$, $g_{*\mathrm{m}}$ and $g_{*\mathrm{M}}$ such that $|f_*| \leqslant f_{*\mathrm{M}}$ and $g_{*\mathrm{m}} \leqslant |g_*| \leqslant g_{*\mathrm{M}}$ where* m *represents minimum of* $*$ *and* M *represents maximum of* $*$; $*$ *denotes V,γ and Q, respectively.*

Assumption 2. [37] *The reference trajectory y_{ref} is sufficiently smooth to t, where y denotes V and h, respectively. In addition, there exist a positive constant B_0 such that $\Omega_0 := \{(y_{\mathrm{ref}}, \dot{y}_{\mathrm{ref}}) | y_{\mathrm{ref}}^2 + \dot{y}_{\mathrm{ref}}^2 \leqslant B_0^2\}$.*

Assumption 3. [16] *The lumped disturbances d_V, d_V, d_V and d_V are bounded satisfying $|d_V| \leqslant d_{V\mathrm{M}}$, $|d_h| \leqslant d_{h\mathrm{M}}$, $|d_\gamma| \leqslant d_{\gamma\mathrm{M}}$ and $|d_Q| \leqslant d_{Q\mathrm{M}}$, where $d_{V\mathrm{M}}$, $d_{h\mathrm{M}}$, $d_{\gamma\mathrm{M}}$ and $d_{Q\mathrm{M}}$ are positive constants.*

Assumption 4. [16] *In view of Eqs. (5) and (6), the input of actuator implicitly appears in HFVs dynamics and there exists a nonlinear relationship between the input and the output of actuator in presence of dead-zone and hysteresis nonlinearities. Taking notice of Fig. 1, we assume that $\upsilon(u)$ satisfies $\upsilon_{\mathrm{m}}u + l_{\mathrm{m}} \leqslant \upsilon(u) \leqslant \upsilon_{\mathrm{M}} + l_{\mathrm{M}}$ and there exist positive constants υ_{m}, υ_{M}, l_{m} and l_{M} such that $\upsilon_{\mathrm{m}} \leqslant \upsilon \leqslant \upsilon_{\mathrm{M}}$ and $l_{\mathrm{m}} \leqslant |l| \leqslant l_{\mathrm{M}}$. From the inequation $\upsilon_{\mathrm{m}}u + l_{\mathrm{m}} \leqslant \upsilon(u) \leqslant \upsilon_{\mathrm{M}} + l_{\mathrm{M}}$, it can be deduced by mean value theorem that*

$$\upsilon(u) = (\sigma\upsilon_{\mathrm{m}} + (1-\sigma)\upsilon_{\mathrm{M}})u + \sigma l_{\mathrm{m}} + (1-\sigma)l_{\mathrm{M}} \tag{7}$$

where σ is a positive function satisfying $0 \leqslant \sigma \leqslant 1$. From Eq. (7), $\upsilon(u)$ can be further written in the following form

$$\upsilon(u) = \upsilon u + l \tag{8}$$

where $\upsilon = \sigma\upsilon_{\mathrm{m}} + (1-\sigma)\upsilon_{\mathrm{M}}$ and $l = \sigma l_{\mathrm{m}} + (1-\sigma)l_{\mathrm{M}}$.

Remark 3. *In the control design of HFVs, input dead-zone and hysteresis are widespread problems that need to be solved urgently due to the wide existence of hydraulic actuator and hinge in HFVs.*[23,35] *It is noting that dead-zone and hysteresis input nonlinearities are non-smooth and the control input appears in the system function as a non-affine form, which makes the controller design quite complex. From Fig. 1, we can see that there exists that $\upsilon_{\mathrm{m}}u + l_{\mathrm{m}} \leqslant \upsilon(u) \leqslant \upsilon_{\mathrm{M}} + l_{\mathrm{M}}$ with respect to dead-zone and hysteresis nonlinearities. Consequently, the dead-zone and hysteresis nonlinearities are transformed into affine form as Eq. (8). In the later controller design, the non-affine forms of input nonlinearity are treated as a linear function by Eq. (8), where υ and l are bounded.*

Lemma 1 [42]. *For any positive constants κ and ι, the following inequality holds*

$$0 \leqslant |\kappa| - \frac{\kappa^2}{\sqrt{\kappa^2 + \iota^2}} \leqslant \iota \tag{9}$$

Lemma 2 [26] (Barbalat Lemma). *For bounded functions $h(t)$ and $\dot{h}(t)$, if $\lim_{t\to\infty}\int_0^t h^2(s)\mathrm{d}s < \infty$, one has*

$$\lim_{t\to\infty} h(t) = 0 \tag{10}$$

The control objection is that V and h can accurately track their own reference trajectories via the proposed adaptive control for HFVs in the presence of the dead-zone and hysteresis input nonlinearities.

3. Adaptive accurate tracking control

3.1. Velocity controller design

The velocity tracking error is defined as

$$e_V = V - V_{\text{ref}} \tag{11}$$

The derivate of e_V is

$$\dot{e}_V = \dot{V} - \dot{V}_{\text{ref}} = f_V + g_V \upsilon(\Phi) + d_V - \dot{V}_{\text{ref}} \tag{12}$$

Define the Lyapunov function candidate:

$$L_{e_V} = \frac{1}{2} e_V^2 \tag{13}$$

Noting Eqs. (8), (12) and (13), we can obtain the derivative of L_{e_V} as

$$\dot{L}_{e_V} = e_V\left(f_V + g_V \upsilon \Phi + g_V l + d_V - \dot{V}_{\text{ref}}\right) \tag{14}$$

From the fact $|f_V| \leqslant f_{V\text{M}}$, $|g_V| \leqslant g_{V\text{M}}$, $|l| \leqslant l_{\text{M}}$, $|d_V| \leqslant d_{V\text{M}}$ and $V_{\text{ref}}^2 + \dot{V}_{\text{ref}}^2 \leqslant B_0^2$, we have

$$|f_V + d_V + g_V l - \dot{V}_{\text{ref}}| \leqslant N_V \tag{15}$$

where $N_V = f_{V\text{M}} + g_{V\text{M}} l_{\text{M}} + d_{V\text{M}} + B_0$ is a unknown bounded positive constant. Besides, we take $\hat{N}_V$ as the estimate of N_V and define $\tilde{N}_V = N_V - \hat{N}_V$.

Construct the actual control law as Eq. (16), the adaptive law is chosen as Eq. (17)

$$\Phi = -n_{V1} k_V e_V - \frac{n_{V1} \varsigma_V \hat{N}_V^2 e_V}{\sqrt{\hat{N}_V^2 e_V^2 + \iota^2(t)}} - n_{V2} c_V e_V \int_0^t e_V \mathrm{d}s \tag{16}$$

$$\dot{\hat{N}}_V = r_V |e_V| \tag{17}$$

where n_{V1} and n_{V2} are the respective signs of g_V and $g_V \int_0^t e_V \mathrm{d}s$; $k_V > 0$, $\varsigma_V > 0$ and $r_V > 0$ are design parameters; $\iota = \iota(t)$ is any positive uniform continuous and bounded function as the following form

$$\lim_{t\to\infty} \int_0^t \iota(s)\mathrm{d}s \leqslant \iota_1 < +\infty, \quad |\dot{\iota}(t)| \leqslant \iota_2 < +\infty \tag{18}$$

Consider the following Lyapunov function candidate

$$L_V = L_{e_V} + \frac{1}{2 r_V} \tilde{N}_V^2 \tag{19}$$

From Eqs. (14)–(17), the derivate of L_V is given as

$$\begin{aligned} \dot{L}_V \leqslant & -n_{V1} k_V g_V \upsilon e_V^2 - \frac{n_{V1} \varsigma_V g_V \upsilon \hat{N}_V^2 e_V^2}{\sqrt{\hat{N}_V^2 e_V^2 + \iota^2}} + |e_V| N_V \\ & - n_{V2} g_V \upsilon c_V e_V^2 \int_0^t e_V \mathrm{d}s - \frac{1}{r_V} \tilde{N}_V \dot{\hat{N}}_V \end{aligned} \tag{20}$$

Choose the design parameter $\varsigma_V \geqslant (g_{V\text{m}} \upsilon_{\text{m}})^{-1}$ and according to Lemma 1 and Assumption 1 ($0 < g_{V\text{m}} \leqslant |g_V|$) and Assumption 4 ($0 < \upsilon_{\text{m}} \leqslant \upsilon$), we have that $g_{V\text{m}} \upsilon_{\text{m}} \leqslant n_{V1} g_V \upsilon$ and $n_{V2} g_V \upsilon c_V e_V^2 \int_0^t e_V \mathrm{d}s \geqslant 0$, then the following inequation holds

$$\begin{aligned} \dot{L}_V &\leqslant -k_V g_{V\text{m}} \upsilon_{\text{m}} e_V^2 + \left(|e_V| \hat{N}_V - \frac{\hat{N}_V^2 e_V^2}{\sqrt{\hat{N}_V^2 e_V^2 + \iota^2}}\right) \\ &\quad - n_{V2} g_V \upsilon c_V e_V^2 \int_0^t e_V \mathrm{d}s \\ &\leqslant -k_V g_{V\text{m}} \upsilon_{\text{m}} e_V^2 + \iota - n_{V2} g_V \upsilon c_V e_V^2 \int_0^t e_V \mathrm{d}s \\ &\leqslant -k_1 e_V^2 + \iota \end{aligned} \tag{21}$$

where $k_1 = k_V g_{V\text{m}} \upsilon_{\text{m}}$.

3.2. Altitude controller design

In this section, the adaptive accurate tracking controllers are developed based on BSC for Eq. (6). The virtual control law χ, the actual control law δ_e and the adaptive law $\hat{N}$ are designed to make the tracking error e accurately converges to zero. The tracking errors of altitude subsystem are defined as following

$$\begin{cases} e_h = h - h_{\text{ref}} \\ e_\gamma = \gamma - \chi_\gamma \\ e_\theta = \theta - \chi_\theta \\ e_Q = Q - \chi_Q \end{cases} \tag{22}$$

The derivate of e_h can be written as

$$\dot{e}_h = \dot{h} - \dot{h}_{\text{ref}} = V\gamma + d_h - \dot{h}_{\text{ref}} \tag{23}$$

Consider the following Lyapunov function candidate

$$L_{e_h} = \frac{1}{2} e_h^2 \tag{24}$$

Then the derivate of L_{e_V} can be obtained as

$$\dot{L}_{e_h} = e_h\left(V\gamma + d_h - \dot{h}_{\text{ref}}\right) \tag{25}$$

Noting that $|d_h| \leqslant d_{h\text{M}}$ and $h_{\text{ref}}^2 + \dot{h}_{\text{ref}}^2 \leqslant B_0^2$, one has

$$|d_h - \dot{h}_{\text{ref}}| \leqslant N_h \tag{26}$$

where $N_h = d_{h\text{M}} + B_0$ is a unknown positive constant. Similarly, $\hat{N}_h$ represents the estimate of N_h and define the estimate error $\tilde{N}_h = N_h - \hat{N}_h$.

Construct the virtual control law and the adaptive law as

$$\chi_\gamma = -k_h e_h - \frac{\varsigma_h \hat{N}_h^2 e_h}{\sqrt{\hat{N}_h^2 e_h^2 + \iota^2}} - n_h c_h e_h \int_0^t e_h \mathrm{d}s \tag{27}$$

$$\dot{\hat{N}}_h = r_h |e_h| \tag{28}$$

where n_h is the sign of $\int_0^t e_h \mathrm{d}s$; $k_h > 0$, $\varsigma_h > 0$ and $r_h > 0$ are design parameters. Consider the following Lyapunov function candidate

$$L_h = L_{e_h} + \frac{1}{2 r_h} \tilde{N}_h^2 \tag{29}$$

Substituting Eqs. (25)–(28) into Eq. (29), then the derivate of L_h is provided as

$$\dot{L}_h \leqslant -k_h V e_h^2 - \frac{\varsigma_h V \hat{N}_h^2 e_h^2}{\sqrt{\hat{N}_h^2 e_h^2 + \iota^2}} + |e_h| \hat{N}_h - n_h c_h e_h^2 \int_0^t e_h \mathrm{d}s \tag{30}$$

Choosing $\varsigma_h \geqslant V^{-1}$ and utilizing Lemma 1, one has

$$\dot{L}_h \leqslant -k_h V e_h^2 + \iota - n_h c_h e_h^2 \int_0^t e_h \mathrm{d}s \leqslant -k_h V e_h^2 + \iota \tag{31}$$

Similarly, we construct the virtual laws as

$$\chi_\theta = -n_{\gamma 1} k_\gamma e_\gamma - \frac{n_{\gamma 1}\varsigma_\gamma \hat{N}_\gamma^2 e_\gamma}{\sqrt{\hat{N}_\gamma^2 e_\gamma^2 + \iota^2}} - n_{\gamma 2} c_\gamma e_\gamma \int_0^t e_\gamma \mathrm{d}s \tag{32}$$

$$\chi_Q = -k_\theta e_\theta - \frac{\hat{N}_\theta^2 e_\theta}{\sqrt{\hat{N}_\theta^2 e_\theta^2 + \iota^2}} - n_\theta c_\theta e_\theta \int_0^t e_\theta \mathrm{d}s \tag{33}$$

where $n_{\gamma 1}$ and $n_{\gamma 2}$ are the respective signs of g_γ and $g_\gamma \int_0^t e_\gamma \mathrm{d}s$, n_θ is the sign of $\int_0^t e_\theta \mathrm{d}s$; In view of Eq. (6), the derivatives of e_γ and e_θ become

$$\dot{e}_\gamma = f_\gamma + g_\gamma \theta + d_\gamma - \dot{\chi}_\gamma, \quad \dot{e}_\theta = Q - \dot{\chi}_\theta \tag{34}$$

In view of Assumptions 1–4, it can be deduced that there exist positive constants N_γ and N_θ such that $|f_\gamma + d_\gamma - \dot{\chi}_\gamma| \leqslant N_\gamma$ and $|\dot{\chi}_\theta| \leqslant N_\theta$ as long as $\dot{\chi}_\gamma$ and $\dot{\chi}_\theta$ are bounded, which is proved in stability analysis. Define $\tilde{N}_\gamma = N_\gamma - \hat{N}_\gamma$, $\tilde{N}_\theta = N_\theta - \hat{N}_\theta$ and the adaptive laws as

$$\dot{\hat{N}}_\gamma = r_\gamma |e_\gamma|, \quad \dot{\hat{N}}_\theta = r_\theta |e_\theta| \tag{35}$$

Define the following Lyapunov function candidate

$$L_\gamma = \frac{1}{2} e_\gamma^2 + \frac{1}{2r_\gamma} \tilde{N}_\gamma^2, \quad L_\theta = \frac{1}{2} e_\theta^2 + \frac{1}{2r_\theta} \tilde{N}_\theta^2 \tag{36}$$

Selecting the design parameter $\varsigma_\gamma \geqslant g_{\gamma \mathrm{m}}^{-1}$, then the following inequalities hold

$$\begin{aligned} \dot{L}_\gamma &\leqslant -k_\gamma g_{\gamma \mathrm{m}} e_\gamma^2 + \iota - n_{\gamma 2} c_\gamma g_\gamma e_\gamma^2 \int_0^t e_\gamma \mathrm{d}s + g_\gamma e_\gamma e_\theta \\ &\leqslant -k_\gamma g_{\gamma \mathrm{m}} e_\gamma^2 + g_\gamma e_\gamma e_\theta + \iota \end{aligned} \tag{37}$$

$$\begin{aligned} \dot{L}_\theta &\leqslant -k_\theta e_\theta^2 + \iota - n_\theta c_\theta e_\theta^2 \int_0^t e_\theta \mathrm{d}s + e_\theta e_Q \\ &\leqslant -k_\theta e_\theta^2 + e_\theta e_Q + \iota \end{aligned} \tag{38}$$

In view of Assumption 1 and with the help of Young's inequation, we have

$$g_\gamma e_\gamma e_\theta \leqslant \frac{1}{2} g_{\gamma \mathrm{M}} e_\gamma^2 + \frac{1}{2} g_{\gamma \mathrm{M}} e_\theta^2 \tag{39}$$

$$e_\theta e_Q \leqslant \frac{1}{2} e_\theta^2 + \frac{1}{2} e_Q^2 \tag{40}$$

In the altitude controller design, the uncertain nonlinearity of actuator is considered, according to Eq. (22), the derivate of e_Q leads to

$$\dot{e}_Q = f_Q + g_Q \upsilon(\delta_\mathrm{e}) + d_Q - \dot{\chi}_Q \tag{41}$$

Consider the Lyapunov function candidate

$$L_{e_Q} = \frac{1}{2} e_Q^2 \tag{42}$$

Considering Eqs. (8), (41) and (42), the derivate of L_{e_Q} is

$$\dot{L}_{e_Q} = e_Q \left(f_Q + g_Q \upsilon \delta_\mathrm{e} + g_Q l + d_Q - \dot{\chi}_Q \right) \tag{43}$$

Then it can be concluded that if $\dot{\chi}_Q$ is bounded, there exist a unknown positive N_Q such that $|f_Q + g_Q l + d_Q - \dot{\chi}_Q| \leqslant N_Q$. Defining $\tilde{N}_Q = N_Q - \hat{N}_Q$, the actual control law and the adaptive law is designed as

$$\delta_\mathrm{e} = -n_{Q1} k_Q e_Q - \frac{n_{Q1}\varsigma_Q \hat{N}_Q^2 e_Q}{\sqrt{\hat{N}_Q^2 e_Q^2 + \iota^2}} - n_{Q2} c_Q e_Q \int_0^t e_Q \mathrm{d}s \tag{44}$$

$$\dot{\hat{N}}_Q = r_Q |e_Q| \tag{45}$$

where n_{Q1} and n_{Q2} are signs of g_Q and $g_Q \int_0^t e_Q \mathrm{d}s$, respectively; k_Q, ς_Q and r_Q are the positive design parameters. Design the following Lyapunov function candidate

$$L_Q = L_{e_Q} + \frac{1}{2r_Q} \tilde{N}_Q^2 \tag{46}$$

Substituting Eqs. (43)–(45) into Eq. (46), we obtain

$$\begin{aligned} \dot{L}_Q \leqslant & -n_{Q1} k_Q g_Q \upsilon e_Q^2 - \frac{n_{Q1}\varsigma_Q g_Q \hat{N}_Q^2 e_Q^2}{\sqrt{\hat{N}_Q^2 e_Q^2 + \iota^2}} + |e_Q| N_Q \\ & - n_{Q2} c_Q e_Q^2 \int_0^t e_Q \mathrm{d}s - \frac{1}{r_Q} \tilde{N}_Q \dot{\hat{N}}_Q \end{aligned} \tag{47}$$

Choosing $\varsigma_Q \geqslant \left(g_{Q\mathrm{m}} \upsilon_\mathrm{m} \right)^{-1}$ and in line accordance with Lemma 1, Eq. (47) results in

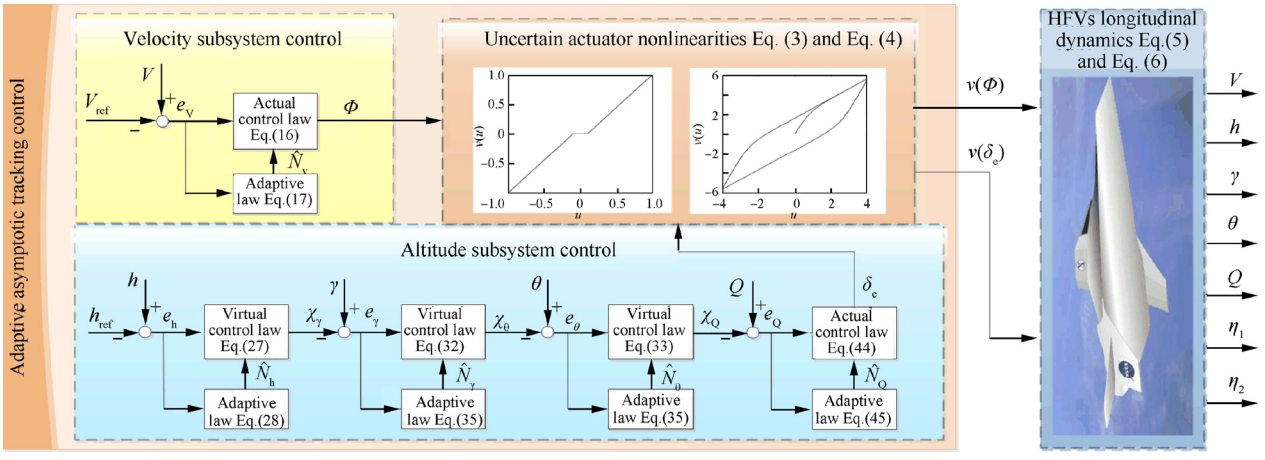

Fig 2 Block diagram of adaptive accurate tracking for HFVs with the actuators dead-zone or hysteresis.

$$\begin{aligned}\dot{L}_Q &\leqslant -k_Q g_{Q\mathrm{m}} \upsilon_{\mathrm{m}} e_Q^2 + \iota - n_{Q2} c_Q e_Q^2 \int_0^t e_Q \mathrm{d}s \\ &\leqslant -k_Q g_{Q\mathrm{m}} \upsilon_{\mathrm{m}} e_Q^2 + \iota\end{aligned} \tag{48}$$

The aforementioned design procedure of the accurate tracking controllers for HFVs can be depicted by a block diagram as shown in Fig. 2.

4. Stability analysis

Theorem 1. *Consider the HFVs model composed by Eqs. (5) and (6), by the virtual control laws Eqs. (27), (32) and (33), by the actual control laws Eqs. (16) and (44), by the adaptive laws Eqs. (17), (28), (35) and (45). Let Assumptions* 1–4 *hold, by choosing appropriate design parameters and giving any* $q > 0$*, if* $L(0) < q$*, then, the inequation* $L(t) \leqslant q$ *holds for* $\forall t > 0$ *and all signals of the closed-loop system are SGUUB. Furthermore, the estimate errors* $\tilde{N}_V$, $\tilde{N}_h$, $\tilde{N}_\gamma$, $\tilde{N}_\theta$ *and* $\tilde{N}_Q$ *stay within the compact sets*

$$\Omega_{\tilde{N}} = \left\{ N_* \in \mathbf{R}^{5\times 1} \middle| \|\tilde{N}_*\| \leqslant p,\ * \in [V, h, \gamma, \theta, Q]^{\mathrm{T}} \right\} \tag{49}$$

where p is a positive constant and the tracking errors e_V and e_h can accurately converge to zero.

Proof. *Construct the Lyapunov function candidate*

$$L = L_h + L_\gamma + L_\theta + L_Q \tag{50}$$

It follows Eqs. (29), (31), (36)–(40), (46) and (48) that the derivate of L can be expressed as

$$\begin{aligned}&L \leqslant -k_h V e_h^2 - \left(k_\gamma g_{\gamma\mathrm{m}} - \tfrac{1}{2} g_{\gamma\mathrm{M}}\right) e_\gamma^2 - \left(k_\theta - \tfrac{1}{2} g_{\gamma\mathrm{M}} - \tfrac{1}{2}\right) e_\theta^2 \\ &-\left(k_Q g_{Q\mathrm{m}} \upsilon_{\mathrm{m}} - \tfrac{1}{2}\right) e_Q^2 + 4\iota \leqslant -k_2 \left(e_h^2 + e_\gamma^2 + e_\theta^2 + e_Q^2\right) + 4\iota\end{aligned} \tag{51}$$

in which $k_2 = \min\left\{k_h V, k_\gamma g_{\gamma\mathrm{m}} - \tfrac{1}{2} g_{\gamma\mathrm{M}}, k_\theta - \tfrac{1}{2} g_{\gamma\mathrm{M}} - \tfrac{1}{2}, k_Q g_{Q\mathrm{m}} \upsilon_{\mathrm{m}} - \tfrac{1}{2}\right\}$ is a positive constant depended on k_h, k_γ, k_θ and k_Q.

Integrating both sides of Eqs. (21) and (51), yields

$$L_V(t) \leqslant L_V(0) - k_1 \int_0^t e_V^2(s)\mathrm{d}s + \int_0^{\mathrm{t}} \iota(\mathrm{s})\mathrm{d}s \leqslant L_V(0) + \iota_1 \tag{52}$$

$$\begin{aligned}L(t) &\leqslant L(0) - k_2 \int_0^t \left(e_h^2 + e_\gamma^2 + e_\theta^2 + e_Q^2\right)\mathrm{d}s + 4\int_0^{\mathrm{t}} \iota(\mathrm{s})\mathrm{d}s \\ &\leqslant L(0) + 4\iota_1\end{aligned} \tag{53}$$

Recalling the definitions of $L_V(t)$ and $L(t)$, we can obtain that e_V, e_h, e_γ, e_θ, e_Q, $\tilde{N}_V$, $\tilde{N}_h$, $\tilde{N}_\gamma$, $\tilde{N}_\theta$ and $\tilde{N}_Q$ are bounded. Consequently, it can be infer that Φ, χ_γ, χ_θ, χ_Q and δ_{e} are bounded. Therefore, all the signals of closed-loop system are bounded. Moreover, from the inequality of Eqs. (52) and (53), we have

$$\int_0^t e_V^2(s)\mathrm{d}s \leqslant \frac{1}{k_1}\left(\mathrm{L}_V(0) + \iota_1\right) < \infty \tag{54}$$

$$\int_0^t \left(e_h^2 + e_\gamma^2 + e_\theta^2 + e_Q^2\right)\mathrm{d}s \leqslant \frac{1}{k_2}\left(\mathrm{L}(0) + 4\iota_1\right) < \infty \tag{55}$$

It follows Lemma 2 that

$$\lim_{t\to\infty} e_V = 0, \quad \lim_{t\to\infty} e_h = 0 \tag{56}$$

Accordingly, the accurate adaptive tracking control for HFVs in the presence of the dead-zone and hysteresis input nonlinearities is achieved. This completes the proof.

Remark 4. *From Eqs. (54) and (55), one has*

$$\int_0^t e_V^2(s)\mathrm{d}s \leqslant \frac{1}{2k_1}\left[e_V^2(0) + \frac{1}{r_V}\tilde{N}_V^2(0) + 2\iota_1\right] \tag{57}$$

$$\int_0^t e_h^2(s)\mathrm{d}s \leqslant \frac{1}{2k_2}\left[e_h^2(0) + \frac{1}{r_h}\tilde{N}_h^2(0) + e_\gamma^2(0) + \frac{1}{r_\gamma}\tilde{N}_\gamma^2(0) + e_\theta^2(0) + \frac{1}{r_\theta}\tilde{N}_\theta^2(0) + e_Q^2(0) + \frac{1}{r_Q}\tilde{N}_Q^2(0) + 8\iota_1\right] \tag{58}$$

where it is concluded that the transient performance lie on the initial errors: $e_V(0)$, $e_h(0)$, $e_\gamma(0)$, $e_\theta(0)$, $e_Q(0)$, the initial estimate errors: $\tilde{N}_V(0)$, $\tilde{N}_h(0)$, $\tilde{N}_\gamma(0)$, $\tilde{N}_\theta(0)$, $\tilde{N}_Q(0)$ and the function $\iota(t)$. Further, it follows that the smaller the initial errors and the initial estimate errors, the better the transient performance. It is worth noting that the time-varying integral function $\iota(t)$ defined in Eqs. (16), (27), (32), (33) and (44) plays a crucial role to analyze the close-loop stability.

5. Simulations

In this section, we demonstrate the proposed adaptive accurate tracking controllers for the longitudinal dynamic model of HFVs Eqs. (1) and (2). The model parameters of HFVs are borrowed from Ref.[36]. It is assumed that HFVs climb a maneuver from the initial trim conditions, listed in Table 1, to the final values $V = 8000$ ft/s (1 ft/s = 0.2048 m/s)and $h = 86000$ ft. The velocity and altitude reference trajectories are through the following filters[13]

$$\frac{V_{\mathrm{ref}}(s)}{V_{\mathrm{c}}(s)} = \frac{0.03^2}{s^2 + 2\times 0.95\times 0.03\times s + 0.03^2} \tag{59}$$

$$\frac{h_{\mathrm{ref}}(s)}{h_{\mathrm{c}}(s)} = \frac{0.03^2}{s^2 + 2\times 0.95\times 0.03\times s + 0.03^2} \tag{60}$$

where $V_{\mathrm{ref}}(s)$ and $h_{\mathrm{ref}}(s)$ represent the inputs of filter, $V_{\mathrm{c}}(s)$ and $h_{\mathrm{c}}(s)$ represent the inputs of filter. The design parameters are set as: $k_V = 1$, $\varsigma_V = 1$, $k_h = k_\gamma = k_\theta = k_Q = 2$, $r_V = r_h = r_\gamma = r_\theta = r_Q = 0.01$, $\varsigma_h = \varsigma_\gamma = \varsigma_\theta = \varsigma_Q = 2$, $c_V = c_h = c_\gamma = c_\theta = c_Q = 0.0001$. The time-varying function is chosen as $\iota(t) = 1/(t^2 + 0.1)$. In order to verify the effectiveness and advantages of the proposed method, the simulation

Table 1 Initial states.

States	Value
V(ft/s)	7700
h(ft)	85000
$\gamma(^\circ)$	0
$\theta(^\circ)$	1.6325
$Q(^\circ)$/s)	0
η_1(ft · slugs$^{0.5}$/ft)	0.97
$\dot{\eta}_1$(ft/s · slugs$^{0.5}$/ft)	0
η_2(ft · slugs$^{0.5}$/ft)	0.7967
$\dot{\eta}_2$(ft/s · slugs$^{0.5}$/ft)	0

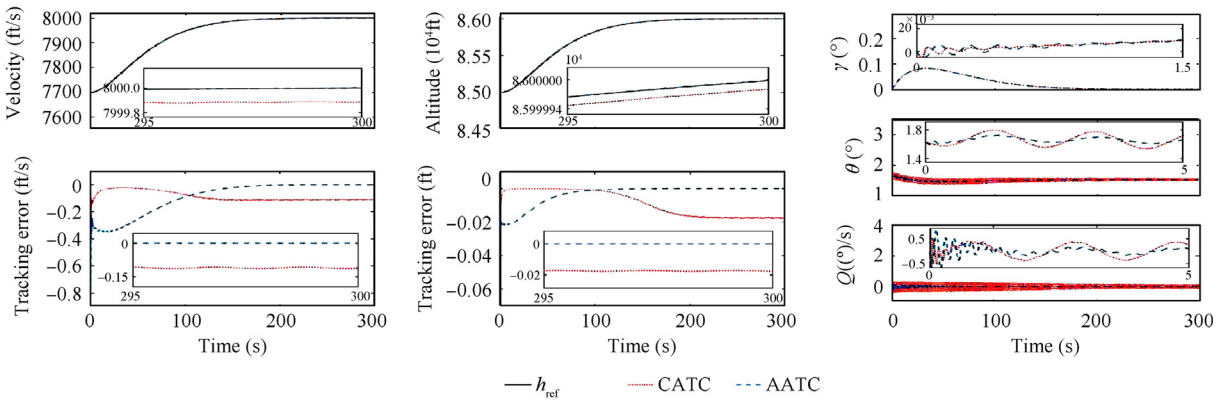

Fig 3 Velocity, altitude tracking performance and attitude angles with actuator dead-zone.

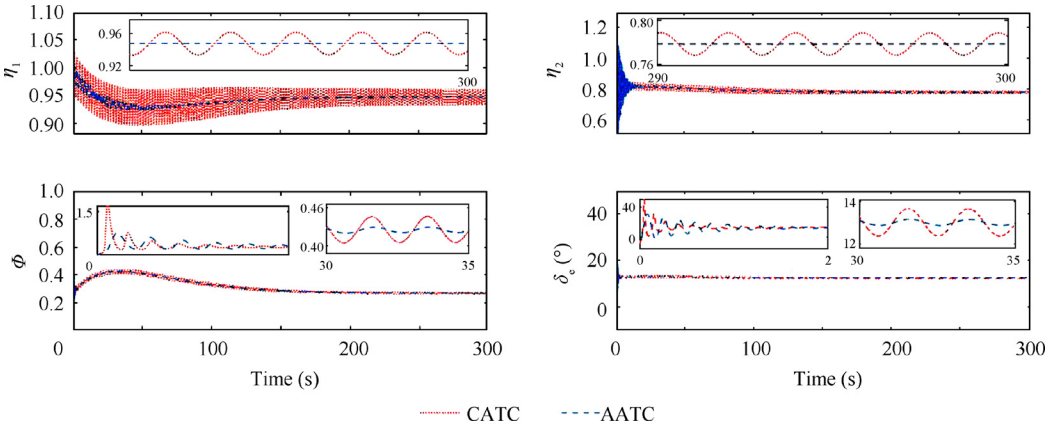

Fig 4 Flexible states and control inputs with actuator dead-zone.

test of the proposed Adaptive Accurate Tracking Control (AATC) is compared with another conventional adaptive tracking control (CATC).[17] The cases of actuators dead-zone and hysteresis are also discussed, respectively.

Case 1. *It is assumed that there exists dead-zone nonlinearity in actuators. The dead-zone models are expressed as*

$$\upsilon(\Phi) = \begin{cases} \Phi - 0.1, & \Phi > 0.1 \\ 0, & \text{others} \end{cases} \tag{61}$$

$$\upsilon(\delta_e) = \begin{cases} \delta_e - 0.1, & \delta_e > 0.1 \\ 0, & -0.1 \leqslant \delta_e \leqslant 0.1 \\ \delta_e + 0.1, & \delta_e < -0.1 \end{cases} \tag{62}$$

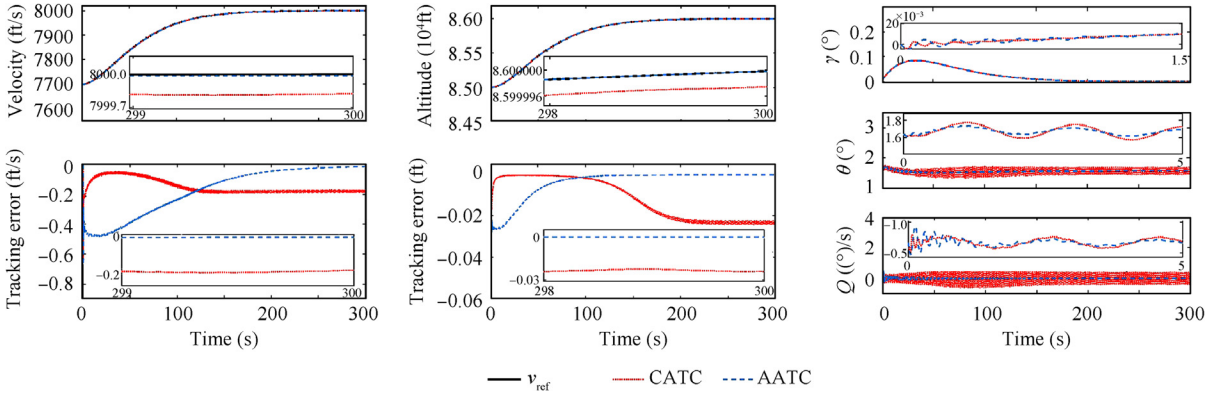

Fig 5 Velocity, altitude tracking performance and attitude angles with actuator hysteresis.

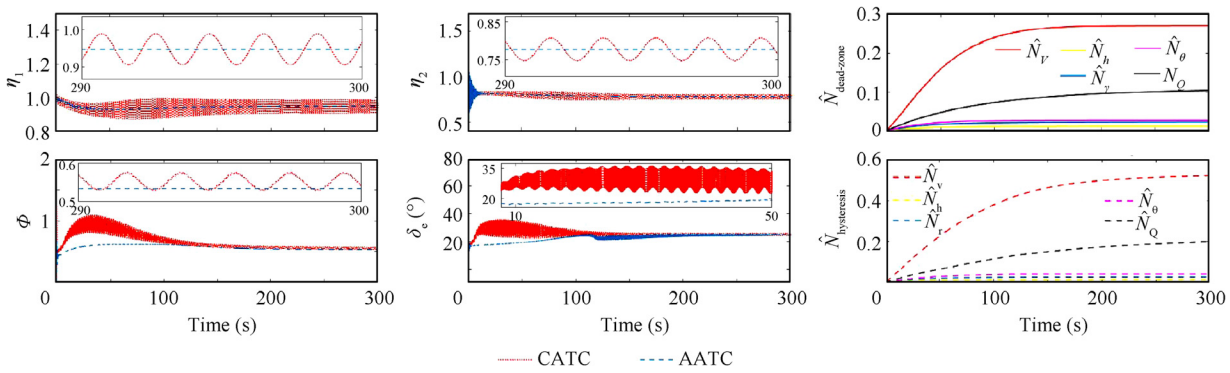

Fig 6 Flexible states and control inputs with actuator hysteresis as well as the value of $\hat{N}$.

The obtained simulation results are depicted in Figs. 3 and 4. Fig. 3 reveals that the accurate tracking (i.e., the tracking errors of velocity and altitude asymptotically converge to zero) via the proposed AATC, while only the bounded error tracking (i.e., the tracking errors of velocity and altitude can converge to a residual set) via CATC. In addition, it can be seen in Figs. 3 and 4 that the AATC proposed in this work has the abilities to deal with the actuator input dead-zone nonlinearities.

It is observed from Figs. 3 and 4 that the attitude angles, flexible states, and control inputs obtained by AATC are smoother than the ones achieved by CATC, and there is no high frequency chattering based on AATC rather than CATC. Thus, the proposed AATC possesses better transient and steady performance.

Case 2. *In this case, the adverse situation that it appears hysteresis nonlinearity in actuators is considered. Consider the following hysteresis functions*

$$\begin{cases} \upsilon(\Phi) = \frac{1}{2}\Phi + \frac{1}{2}\ell \\ \dot{\ell} = \dot{\Phi} - 0.3|\dot{\Phi}| - 0.05\dot{\Phi}|\ell| \end{cases} \tag{63}$$

$$\begin{cases} \upsilon(\delta_e) = \frac{1}{2}\delta_e + \frac{1}{2}\ell \\ \dot{\ell} = \dot{\delta}_e - 0.3|\dot{\delta}_e| - 0.05\dot{\delta}_e|\ell| \end{cases} \tag{64}$$

Simulation results are presented in Figs. 5 and 6. From Fig. 5, it can be shown in Fig. 5 that the accurate tracking (tracking errors converge to zero) is obtained base on AATC rather than CATC, while CATC achieves bounded tracking errors. It can be observed from Figs. 5 and 6 that AATC has the capabilities to handle with actuator hysteresis. Moreover, it is seen that smoother trajectories of the attitude angles, the flexible states and the control inputs are achieved by AATC. Thereby the transient and steady performance of the exploited control strategy is better via AATC when the actuator hysteresis is taken into account. Further, the proposed AATC overcomes the shortcoming of high frequency oscillation issue. In addition, the adaptive parameter values of the devised AATC, both in the dead-zone and hysteresis condition, are bounded, as depicted in Fig. 6.

6. Conclusions

In this work, a novel adaptive accurate tracking controller, capable of coping with non-affine form of actuator nonlinearities such as dead-zone and hysteresis, is exploited for the longitudinal model of an HFVs effected by external disturbances. To overcome this barrier, non-affine form of actuator nonlinearity is transformed into affine form via mean value theorem. By means of a new back-stepping adaptive design, the velocity and altitude can accurately converge to zero in spite of actuator dead-zone and hysteresis. Besides, all signals of the closed-loop system are guaranteed to be SGUUB. Finally, the effectiveness and superiority of the proposed approach are verified by simulation results.

Declaration of Competing Interest

The authors declare that they have no known competing financial interests or personal relationships that could have appeared to influence the work reported in this paper.

Acknowledgment

This work is supported by the Natural Science Basic Research Program of Shaanxi Province, China (No. 2019JQ-711).

References

1. Li HF, Lin P, Xu DJ. Control-oriented modeling for air-breathing hypersonic vehicle using parameterized configuration approach. *Chin J Aeronaut* 2011;**24**(1):81–9.
2. Chen BY, Liu YB, Shen HD, et al. Performance limitations in trajectory tracking control for air-breathing hypersonic vehicles. *Chin J Aeronaut* 2018;**32**(1):170–8.
3. Zhu JJ, Wang XJ, Zhang HG, et al. Six sigma robust design optimization for thermal protection system of hypersonic vehicles based on successive response surface method. *Chin J Aeronaut* 2019;**32**(9):2095–108. https://doi.org/10.1016/j.cja.2019.04.009 [in press].
4. Liu Y, Dong CY, Zhang WQ, et al. Phase plane design based fast altitude tracking control for hypersonic flight vehicle with angle of attack constraint. Chin J Aeronaut 2020. Available from: https://doi.org/10.1016/j.cja.2020.04.026 [in press].

5. Li ZY, Zhou WJ, Liu H. Robust controller design of non-minimum phase hypersonic aircrafts model based on quantitative feedback theory. *J Astronaut Sci* 2019;**67**:137–63.
6. Hu XX, Xu B, Hu CH. Robust adaptive fuzzy control for HFV with parameter uncertainty and unmodeled dynamics. *IEEE Trans Ind Electron* 2018;**65**(11):8851–60.
7. Xu B, Wang DW, Zhang YM, et al. DOB-based neural control of flexible hypersonic flight vehicle considering wind effects. *IEEE Trans Ind Electron* 2017;**64**(11):8676–85.
8. Basin MV, Yu P, Shtessel YB. Hypersonic missile adaptive sliding mode control using finite- and fixed-time observers. *IEEE Trans Ind Electron* 2017;**65**(1):930–41.
9. Wu YJ, Zuo JX, Sun LH. Adaptive terminal sliding mode control for hypersonic flight vehicles with strictly lower convex function based nonlinear disturbance observer. *ISA Trans* 2017;**71**(2):215–26.
10. Hu QL, Meng Y. Adaptive backstepping control for air-breathing hypersonic vehicle with actuator dynamics. *Aerosp Sci Technol* 2017;**67**:412–21.
11. Xu B, Shou YX. Composite learning control of MIMO systems with applications. *IEEE Trans Ind Electron* 2018;**65**(8):6414–24.
12. Liu JX, An H, Gao YB, et al. Adaptive control of hypersonic flight vehicles with limited angle-of-attack. *IEEE Trans Mechatron* 2018;**23**(2):883–94.
13. Bu XW, Wu XY, Zhu FJ, et al. Novel prescribed performance neural control of a flexible air-breathing hypersonic vehicle with unknown initial errors. *ISA Trans* 2015;**59**:149–59.
14. Bu XW, Xiao Y, Wang K. A prescribed performance control approach guaranteeing small overshoot for air-breathing hypersonic vehicles via neural approximation. *Aerosp Sci Technol* 2017;**71**:485–98.
15. Bu XW. Air-breathing hypersonic vehicles funnel control using neural approximation of non-affine dynamics. *IEEE/ASME Trans Mechatron* 2018;**23**(5):2099–108.
16. Xu B. Robust adaptive neural control of flexible hypersonic flight vehicle with dead-zone input nonlinearity. *Nonlinear Dyn* 2015;**80**(3):1509–20.
17. Gou YY, Li HB, Dong XM, et al. Constrained adaptive neural network control of an MIMO aeroelastic system with input nonlinearities. *Chin J Aeronaut* 2017;**30**(2):796–806.
18. Sun HB, Li SH, Sun CY. Adaptive fault-tolerant controller design for airbreathing hypersonic vehicle with input saturation. *J Syst Eng Electron* 2013;**24**(3):488–99.
19. Zhao XD, Shi P, Zheng XL, et al. Adaptive tracking control for switched stochastic nonlinear systems with unknown actuator dead-zone. *Automatica* 2015;**60**:193–200.
20. Shahnazi R, Haghani A, Jeinsch T. Adaptive fuzzy observer-based stabilization of a class of uncertain time-delayed chaotic systems with actuator nonlinearities. *Chaos, Solitons Fractals* 2015;**76**:98–110.
21. Lv ML, Baldi S, Liu ZC. The non-smoothness problem in disturbance observer design: A set-invariance based adaptive fuzzy control method. *IEEE Trans Fuzzy Syst* 2019;**27**(3):598–604.
22. Zong Q, Wang F, Tian BL, et al. Robust adaptive dynamic surface control design for a flexible air-breathing hypersonic vehicle with input constraints and uncertainty. *Nonlinear Dyn* 2014;**78**(1):289–315.
23. Wang YY, Hu JB. Improved prescribed performance control for air-breathing hypersonic vehicles with unknown dead-zone input nonlinearity. *ISA Trans* 2018;**79**:95–107.
24. Du YL, Sun DY, Fu J, et al. Adaptive maneuver control of hypersonic reentry flight via self-organizing recurrent functional link network. *IEEE international joint conference on neural networks*; 2016.
25. Shi Z, Wang F, Ma WQ. Control of hypersonic vehicle based on improved QFT; *Fifth international symposium on computational intelligence & design*; 2012.
26. Liu YH. Dynamic surface asymptotic tracking of a class of uncertain nonlinear hysteretic systems using adaptive filters. *J Franklin Inst* 2018;**355**(1):123–40.
27. Wei JL, Liu ZC. Asymptotic tracking control for a class of pure-feedback nonlinear systems. *IEEE Access* 2019;**7**:166721–8.
28. Lv ML, Schutter BD, Yu WW, et al. Adaptive asymptotic tracking for a Class of Uncertain switched positive compartmental models with application to anesthesia. *IEEE Transactions on Systems, Man, and Cybernetics: Systems* 2019. Available from: https://doi.org/10.1109/TSMC.2019.2945590 [in press].
29. Lv ML, Schutter DB, Yu WW, et al. Nonlinear systems with uncertain periodically disturbed control gain functions: adaptive fuzzy control with invariance properties. *IEEE Trans Fuzzy Syst* 2020;**28**(4):746–57.
30. Lv ML, Yu WW, Baldi S. The set-invariance paradigm in fuzzy adaptive DSC design of large-scale nonlinear input-constrained systems. *IEEE Transactions on Systems, Man, and Cybernetics: Systems* 2019. Available from: https://doi.org/10.1109/TSMC.2019.2895101 [in press].
31. Zuo RW, Dong XM, Chen Y, et al. Adaptive neural control for a class of non-affine pure-feedback nonlinear systems. *Int J Control* 2019;**92**(6):1354–66.
32. Bu XW, Wu XY, Ma Z, et al. Novel adaptive neural control of flexible air-breathing hypersonic vehicles based on sliding mode differentiator. *Chin J Aeronaut* 2015;**28**(4):1209–16.
33. Liu ZC, Dong XM, Xue JP, et al. Adaptive neural control for a class of pure-feedback nonlinear systems via dynamic surface technique. *IEEE Trans Neural Networks Learn Syst* 2016;**27**(9):1969–75.
34. Hu QL, Meng Y, Wang CL, et al. Adaptive backstepping control for air-breathing hypersonic vehicles with input nonlinearities. *Aerosp Sci Technol* 2018;**73**:289–99.
35. Guo YY, Xu B, Hu XX, et al. Two controller designs of hypersonic flight vehicle under actuator dynamics and AOA constraint. *Aerosp Sci Technol* 2018;**80**:11–9.
36. Parker JT, Serrani A, Yurkovich S, et al. Control-oriented modeling of an air-breathing hypersonic vehicle. *J Guidance Control Dyn* 2007;**30**(3):856–69.
37. Sun JL, Yi JQ, Pu ZQ, et al. Fixed-time sliding mode disturbance observer-based nonsmooth backstepping control for hypersonic vehicles. *IEEE Transactions on Systems, Man, and Cybernetics: Systems* 2018. Available form: https://doi.org/10.1109/TSMC.2018.2847706 [in press].
38. Liu ZC, Dong XM, Xue JP, et al. Adaptive neural control for a class of time-delay systems in the presence of backlash or dead-zone nonlinearity. *IET Control Theory Appl* 2014;**8**(11):1009–22.
39. Nidhal C, Hamid B, Hichem A. Adaptive fuzzy PID control for a class of uncertain MIMO nonlinear systems with dead-zone inputs nonlinearities. *Iran J Sci Technol Trans Electr Eng* 2018;**42**(1):1–19.
40. Xu B, Yang CG, Pan YP. Global neural dynamic surface tracking control of strict-feedback systems with application to hypersonic flight vehicle. *IEEE Trans Neural Networks Learn Syst* 2015;**26**(10):2563–75.
41. Fiorentini L, Serrani A, Bolender MA, et al. Nonlinear robust adaptive control of flexible air-breathing hypersonic vehicles. *J Guidance Control Dyn* 2009;**32**(2):401–16.
42. Wang CL, Zuo ZY. Adaptive trajectory tracking control of output constrained multi-rotors systems. *IET Control Theory Appl* 2014;**8**(13):1163–74.